A Geometric Analysis of Neural Collapse with Unconstrained Features

Zhihui Zhu[*]
University of Denver
zhihui.zhu@du.edu

Tianyu Ding
Johns Hopkins University
tding1@jhu.edu

Jinxin Zhou
University of Denver
jinxin.zhou@du.edu

Xiao Li
University of Michigan
xlxiao@umich.edu

Chong You
Google Research
cyou@google.com

Jeremias Sulam
Johns Hopkins University
jsulam1@jhu.edu

Qing Qu
University of Michigan
qingqu@umich.edu

Abstract

We provide the first global optimization landscape analysis of *Neural Collapse*— an intriguing empirical phenomenon that arises in the last-layer classifiers and features of neural networks during the terminal phase of training. As recently reported in [1], this phenomenon implies that *(i)* the class means and the last-layer classifiers all collapse to the vertices of a Simplex Equiangular Tight Frame (ETF) up to scaling, and *(ii)* cross-example within-class variability of last-layer activations collapses to zero. We study the problem based on a simplified *unconstrained feature model*, which isolates the topmost layers from the classifier of the neural network. In this context, we show that the classical cross-entropy loss with weight decay has a benign global landscape, in the sense that the only global minimizers are the Simplex ETFs while all other critical points are strict saddles whose Hessian exhibit negative curvature directions. Our analysis of the simplified model not only explains what kind of features are learned in the last layer, but also shows why they can be efficiently optimized, matching the empirical observations in practical deep network architectures. These findings provide important practical implications. As an example, our experiments demonstrate that one may set the feature dimension equal to the number of classes and fix the last-layer classifier to be a Simplex ETF for network training, which reduces memory cost by over 20% on ResNet18 without sacrificing the generalization performance. The source code is available at https://github.com/tding1/Neural-Collapse.

1 Introduction

In the past decade, the revival of deep neural networks (DNN) has led to dramatic success in numerous applications ranging from computer vision, to natural language processing, to scientific discovery and beyond [2–5]. Nevertheless, the practice of deep networks has been shrouded with mystery as our theoretical understanding for the success of deep learning remains elusive. There are many intriguing phenomena, such as implicit algorithmic bias in training [6–10], and good generalization of highly-overparameterized networks [7, 11–15], that seem often contradictory to, or cannot be explained by, classical optimization and learning theory.

[*]The first two authors contributed to this work equally.

35th Conference on Neural Information Processing Systems (NeurIPS 2021).

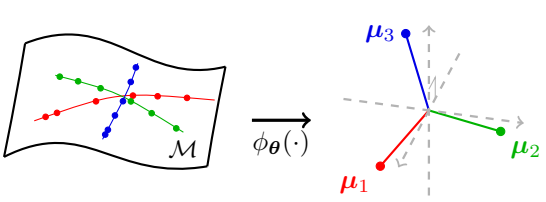

Figure 1: Illustration of Neural Collapse. Here $\phi_{\boldsymbol{\theta}}(\cdot)$ denotes the feature mapping of the network, i.e. the output of the penultimate layer; see (1) for the formal definition.

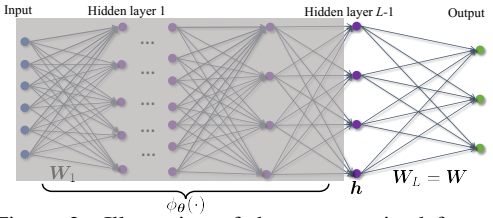

Figure 2: Illustration of the unconstrained feature model, where the gray box is peeled off so that the representation $\boldsymbol{h}$ is modeled by a simple decision variable for every training sample.

Towards demystifying DNN, recent seminal work [1, 16] empirically discovered an intriguing phenomenon that persists across a range of canonical classification problems during the terminal phase of training. As illustrated in Figure 1, it has been widely observed that last-layer features and classifiers of a trained DNN exhibit simple but elegant mathematical structures:

- ***Variability Collapse*:** cross-example within-class variability of last-layer features collapses to zero, as the individual features of each class themselves concentrate to their isolated class-means.
- ***Convergence to Simplex ETF*:** the class-means centered at their global mean are not only linearly separable, but are actually maximally distant and located on a sphere centered at the origin up to scaling (i.e., they form a Simplex Equiangular Tight Frame (ETF) – or Simplex ETF, which is formally defined in Definition C.1 in the Appendix).
- ***Convergence to Self-duality*:** the last-layer linear classifiers, living in the dual vector space to that of the class-means, are perfectly matched with their class-means.
- ***Simple Decision Rule*:** the last-layer classifier is behaviorally equivalent to a Nearest Class-Center decision rule.

These results suggest that deep networks are learning maximally separable features between classes, and a max-margin classifier in the last layer upon these learned features, touching the ceiling in terms of the performance. This phenomenon is referred to as *Neural Collapse* ($\mathcal{NC}$) [1], and it persists across a range of canonical classification problems, on different neural network architectures (e.g., VGG [17], ResNet [18], and DenseNet [19]) and on a variety of standard datasets (such as MNIST [20], CIFAR [21], and ImageNet [22]).

Fully demystifying the $\mathcal{NC}$ phenomenon in theory can be very challenging. Perhaps the most difficult hurdle lies in the nonconvexity of the optimization problem for training neural networks, which, loosely speaking, stems from the nonlinear interaction across many different layers of neural networks. Towards this goal, a recent line of work [23–29] studied the properties of last-layer classifiers and features based on the assumption of the so-called *unconstrained feature model* [23] or *layer-peeled model* [26]. At a high level, the unconstrained feature model takes a *top-down* approach to the analysis of deep neural networks [23–26, 29–31], wherein the last-layer features are modeled as *free* optimization variables (hence we call them *unconstrained features*) along with the last-layer classifiers (see Figure 2 for an illustration); this is in contrast to the conventional *bottom-up* approach that studies the problem starting from the input [32–42].[2] The underlying reasoning is that modern deep networks are often highly overparameterized with the capacity of learning any representations [43–46], so that the last-layer features can approximate, or interpolate, any point in the feature space. In this way, the model simplifies the study of last-layer features, enabling us to analyze the interaction between them and the last-layer classifiers.

Nonetheless, the simplified unconstrained feature model still leaves us a highly nonconvex training loss to be dealt with. Despite the nonconvexity, recent work [23–28] studied the global minimizers, proving that Simplex ETFs (i.e., $\mathcal{NC}$) are indeed global solutions to the nonconvex loss. In particular, the work [23, 47] studied the training problem with the least-squared loss, proving that the gradient flow converges to $\mathcal{NC}$ solutions with extra assumptions. Another line of work [24–27] considered the commonly used cross-entropy loss for classification, showing that the only global minimizers of the loss function are Simplex ETFs with different constraints on the weights and features.[3] However,

[2] Here, top-down means that we study the network starting from the last-layer down to the input layer, whereas bottom-up refers to an approach from the input up to the last layer.

[3] The constraints on the features are mainly used to prevent it from approaching infinity since the objective function, with the cross-entropy loss, is not coercive. Note that we still refer to this model as an *unconstrained feature model* even if they include norm constraints or regularization.

Table 1: Comparison of the setup and results under the unconstrained feature model with cross-entropy loss.

	Regularizer		Bias term	Results	
	Constraint	Weight decay		Global minimizer	Landscape
[24–27]	✓			✓	
This paper		✓	✓	✓	✓

these results still suffer from several limitations: *(i)* due to the nonconvex nature, only characterizing optimality conditions is not enough to explain the empirical convergence of iterative algorithms to $\mathcal{NC}$, such as stochastic gradient descent (SGD); *(ii)* the problem formulations differ from those typically used in practice, which deploy norm regularization (i.e., weight decay) on the weights, rather than enforcing constraints, for the ease of optimization.[4]

Contributions of This Work. Inspired by these pioneering results [1, 23–26, 29], in this work we take a step further by characterizing the global optimization landscape of the network training loss based on the unconstrained feature model. Our contributions are summarized as follows.

- ***Benign Global Landscape.*** For the unconstrained feature model, we provide the first result showing that a commonly used, regularized cross-entropy loss is a *strict saddle function* [49–51]. In other words, every critical point is either a global solution (corresponding to Simplex ETFs) or a *strict saddle point*[5] with negative curvature, so that there is *no* spurious local minimizer on the optimization landscape. As summarized in Table 1, this is in contrast to previous work [23–26] that only characterizes global minimizers.
- ***Efficient, Algorithmic Independent, Global Optimization.*** The benign global landscape implies that any method that can escape strict saddle points (e.g. stochastic gradient descent) converges to a global solution [52] that exhibits $\mathcal{NC}$. This result supports our empirical observation, as shown in Section 4.1, that practical overparameterized networks always converge to Simplex ETF solutions with a diverse choice of optimization algorithms.
- ***Cost Reduction for Practical Network Training.*** Moreover, the universality of $\mathcal{NC}$ implies that there is no need of training the last-layer classifiers since the weights can be simply fixed as a Simplex ETF throughout the training process. On the other hand, since $\mathcal{NC}$ happens whenever $d \geq K$, this implies that we can choose the feature dimension d comparable to the number of classes K, reducing the feature dimension for further computational benefits. In Section 4.3, our experiments demonstrate that such a strategy achieves on par performance with classical training methods, leading to substantial cost reductions on both memory and computation.

Our results shed new light on the question raised in the recent paper [53] on the role of the optimization strategy (e.g., stochastic gradient descent) for achieving $\mathcal{NC}$ in training practical deep networks. This question also relates to the recent highly influential work [7] on the implicit algorithmic bias. For multi-class classification problems with linearly separable data, this work [7] showed that linear predictors optimized by gradient descent converge to the max-margin classifiers even without adding any explicit regularization on the cross-entropy loss. Based on this result, a sequence of works [54–61] laid great emphasis on the notion of "inductive bias" of particular optimization algorithms as a reason for the surprising success in training deep learning models.[6] In contrast, both our theoretical result on the global landscape for the unconstrained feature model and the empirical evidence on practical deep models demonstrate that $\mathcal{NC}$ in network training is facilitated *not only* by the choice of the optimization methods, but more importantly, by the choice of loss functions and the power of overparameterization in the network architecture.

2 The Problem Setup

A deep neural network is essentially a *nonlinear* mapping $\psi(\cdot) : \mathbb{R}^D \mapsto \mathbb{R}^K$, which can be modeled by a composition of simple maps: $\psi(\boldsymbol{x}) = \psi^L \circ \cdots \circ \psi^2 \circ \psi^1(\boldsymbol{x})$ for $\boldsymbol{x} \in \mathbb{R}^D$, where $\psi^\ell(\cdot)$ $(1 \leq \ell \leq L)$ are called "layers". Each layer is composed of an affine transform, represented by

[4] A recent concurrent work [48] studied the gradient flow as well as landscape of the cross-entropy loss under the unconstrained feature model, but without using any constraints or regularizers on the weights.

[5] Throughout the paper, for a minimization problem, we will not distinguish between local maxima and saddle points. We call a critical point *strict saddle* if the Hessian at this point has at least one negative eigenvalue.

[6] While (stochastic) gradient descent and generic steepest descent methods can converge to max-margin classifiers, it should be noted that other commonly used optimization algorithms in deep learning, such as AdaGrad [62] and Adam [63], do not have max-margin properties in general and their solutions depend upon initialization, step-size and other algorithm hyper-parameters [64–66].

some weight matrix $\boldsymbol{W}_\ell$, and bias $\boldsymbol{b}_\ell$, followed by a simple *nonlinear*[7] activation function $\sigma(\cdot)$. More precisely, a vanilla L-layer neural network can be written as

$$\psi_{\boldsymbol{\Theta}}(\boldsymbol{x}) \;=\; \boldsymbol{W}_L \underbrace{\sigma\left(\boldsymbol{W}_{L-1}\cdots\sigma\left(\boldsymbol{W}_1\boldsymbol{x}+\boldsymbol{b}_1\right)+\boldsymbol{b}_{L-1}\right)}_{\phi_{\boldsymbol{\theta}}(\boldsymbol{x})}+\boldsymbol{b}_L. \tag{1}$$

For convenience, we use $\boldsymbol{\Theta} = \{\boldsymbol{W}_k, \boldsymbol{b}_k\}_{k=1}^{L}$ to denote *all* the network parameters, and use $\boldsymbol{\theta} = \{\boldsymbol{W}_k, \boldsymbol{b}_k\}_{k=1}^{L-1}$ to denote the network parameters up to the last layer. The output of the penultimate layer, denoted by $\phi_{\boldsymbol{\theta}}(\boldsymbol{x})$, is usually referred to as the *representation* or *feature* of the input $\boldsymbol{x}$ learned from the network. In this way, the function implemented by a neural network classifier can also be expressed as a linear classifier acting upon $\phi_{\boldsymbol{\theta}}(\boldsymbol{x})$.

The goal of deep learning is to fit the parameters $\boldsymbol{\Theta}$ so that the output of the model on an input samples $\boldsymbol{x}$ approximates the corresponding output $\boldsymbol{y}$, i.e. so that $\psi_{\boldsymbol{\Theta}}(\boldsymbol{x}) \approx \boldsymbol{y}$, in expectation over a distribution of input-output pairs, $\mathcal{D}$. This can be achieved by optimizing an appropriate loss function $\mathcal{L}(\psi_{\boldsymbol{\Theta}}(\boldsymbol{x}), \boldsymbol{y})$ which quantifies this approximation. In this work, we focus on multi-class classification tasks (say, with K classes), where the class label of a sample $\boldsymbol{x}$ is given by a one-hot vector $\boldsymbol{y} \in \mathbb{R}^K$ representing its membership to one of the K classes. In this setting, cross-entropy is one of the most popular choices for the loss function. Naturally, the distribution $\mathcal{D}$ is unknown, but we have access to training samples that are drawn i.i.d. from $\mathcal{D}$. In this way, one can minimize the empirical risk over these samples by optimizing the following problem

$$\min_{\boldsymbol{\Theta}} \sum_{k=1}^{K}\sum_{i=1}^{n_k} \mathcal{L}_{\mathrm{CE}}\left(\psi_{\boldsymbol{\Theta}}(\boldsymbol{x}_{k,i}), \boldsymbol{y}_k\right) \;+\; \frac{\lambda}{2}\left\|\boldsymbol{\Theta}\right\|_F^2, \tag{2}$$

where $\boldsymbol{y}_k \in \mathbb{R}^K$ is a one-hot vector with only the kth entry equal to unity ($1 \le k \le K$), $\{n_k\}_{k=1}^{K}$ are the numbers of training samples in each class, and $\lambda > 0$ is the regularization parameter (or weight decay penalty), and $\mathcal{L}_{\mathrm{CE}}(\cdot,\cdot)$ is the cross-entropy loss. As introduced in Section 1, recent work [1] showed that the features learned by minimizing the above objective showcase the $\mathcal{NC}$ phenomenon: their within-class variability vanishes, and the features converge to a Simplex ETF.

2.1 Problem Formulation Based on Unconstrained Feature Models

In deep network models, the nonlinearity and interaction between a large number of layers results in tremendous challenges for analyzing this learning problem. Since modern networks are often highly overparameterized to approximate any continuous function and the characterization of $\mathcal{NC}$ only involves the last-layer features $\phi_{\boldsymbol{\theta}}(\boldsymbol{x})$, a natural idea to simplify the analysis is to treat these features as free optimization variables $\boldsymbol{h} = \phi_{\boldsymbol{\theta}}(\boldsymbol{x}) \in \mathbb{R}^d$, which motivates the name *unconstrained feature model*[8] [23] (see Figure 2 for an illustration). In this way, we can rewrite the network output as $\psi_{\boldsymbol{\Theta}}(\boldsymbol{x}) = \boldsymbol{W}_L\boldsymbol{h} + \boldsymbol{b}_L$.

For simplicity, we consider the setting where the number of training samples in each class is balanced (i.e., $n_k = n$ for all $k \in [K] := \{1, 2, \ldots, K\}$). We also write $\boldsymbol{W} = \boldsymbol{W}_L$ and $\boldsymbol{b} = \boldsymbol{b}_L$ for conciseness. Based on the unconstrained feature model, we consider a slight variant of (2), given by

$$\min_{\boldsymbol{W},\boldsymbol{H},\boldsymbol{b}} f(\boldsymbol{W},\boldsymbol{H},\boldsymbol{b}) := \frac{1}{Kn}\sum_{k=1}^{K}\sum_{i=1}^{n}\mathcal{L}_{\mathrm{CE}}\left(\boldsymbol{W}\boldsymbol{h}_{k,i}+\boldsymbol{b}, \boldsymbol{y}_k\right) + \frac{\lambda_{\boldsymbol{W}}}{2}\left\|\boldsymbol{W}\right\|_F^2 + \frac{\lambda_{\boldsymbol{H}}}{2}\left\|\boldsymbol{H}\right\|_F^2 + \frac{\lambda_{\boldsymbol{b}}}{2}\left\|\boldsymbol{b}\right\|_2^2, \tag{3}$$

with $\boldsymbol{W} \in \mathbb{R}^{K\times d}$, $\boldsymbol{H} = [\boldsymbol{h}_{1,1}\cdots\boldsymbol{h}_{K,n}] \in \mathbb{R}^{d\times N}$ (here, we denote $N = nK$), $\boldsymbol{b} \in \mathbb{R}^K$, and $\lambda_{\boldsymbol{W}}, \lambda_{\boldsymbol{H}}, \lambda_{\boldsymbol{b}} > 0$ are the penalty parameters for the weight decay.

As summarized in Table 1, similar optimization problems have been considered in [24–26]. In contrast to these, our problem formulation here (3), with bias and weight decay, is closer to the loss used in practice for training neural networks; existing work [24–26] considered constrained[9] variants of (3) and without the bias term, which can be implemented but seldom used in practice due to the difficulty of optimization. In the following, we briefly discuss the differences between our simplification and practical settings for training neural networks.

[7] The nonlinear operator may include activations such as ReLU [67], pooling, and normalization [68], etc.

[8] This model is also called *layer-peeled model* in [26], where one "peels" off the first $L-1$ layers. It has also been recently studied in [24, 25]. Throughout the paper, we will simply call it unconstrained feature model.

[9] For example, the work [26] considers inequality constraints such that the energy of $\boldsymbol{W}$ and $\boldsymbol{H}$ are bounded; the other work [24, 25] enforces $\boldsymbol{W}$ and $\boldsymbol{H}$ on the spheres up to scaling.

- **Weight Decay on $\boldsymbol{W}$ and $\boldsymbol{H}$.** One simplification of our formulation is in the weight decay. In practice, weight decay is usually imposed on the network parameters $\boldsymbol{\Theta}$, while we enforce weight decay on the last layer's classifier, $\boldsymbol{W}$, and features, $\boldsymbol{H}$. However, this idealization is reasonable since the energy of the features (i.e., $\|\boldsymbol{H}\|_F$) can indeed be upper bounded by the energy of the weights at every layer if the inputs are bounded (which holds in practice), implying that the norm of $\boldsymbol{H}$ is *implicitly* penalized by penalizing $\boldsymbol{\Theta}$. Our experiments in the Appendix demonstrate that both approaches exhibit similar $\mathcal{NC}$ phenomena and comparable performance in practice.
- **Treating the Last-layer Features as Optimization Variables.** One may question that "peeling off" the $L-1$ layers might oversimplify the problem. Nonetheless, this simplification (which is also adopted in [23–26]) is based on the fact that neural networks with sufficient overparameterization can approximate any function – in Section 4.2, we numerically demonstrate that $\mathcal{NC}$ persists even when we train overparametrized networks on randomly generated labels. Moreover, as we shall see in the following sections, both our theory and experiments demonstrate that our simplification preserves the core properties of last-layer classifiers and features during training – the $\mathcal{NC}$ phenomenon. More specifically, in Section 3 we show that Simplex ETFs are the only global minimizers to our simplified loss function (3), and the loss function is a strict saddle function with no other spurious local minimizers so that it can be optimized efficiently to global optimality.

3 Main Theoretical Results

In this section, we present our study on global optimality conditions as well as the optimization landscape of the nonconvex loss in (3).

Theorem 3.1 (Global Optimality Conditions) *Assume that the feature dimension d is no smaller than the number of classes K, i.e. $d \geq K-1$, and the number of training samples in each class is balanced, $n = n_1 = \cdots = n_K$. Then any global minimizer $(\boldsymbol{W}^\star, \boldsymbol{H}^\star, \boldsymbol{b}^\star)$ of f in (3) satisfies*

$$
\begin{aligned}
&w^\star := \left\|\boldsymbol{w}^{\star 1}\right\|_2 = \left\|\boldsymbol{w}^{\star 2}\right\|_2 = \cdots = \left\|\boldsymbol{w}^{\star K}\right\|_2, \quad \text{and} \quad \boldsymbol{b}^\star = b^\star \mathbf{1}, \\
&\boldsymbol{h}^\star_{k,i} = \sqrt{\frac{\lambda_{\boldsymbol{W}}}{\lambda_{\boldsymbol{H}} n}}\boldsymbol{w}^{\star k}, \quad \forall\, k \in [K],\ i \in [n], \quad \text{and} \quad \overline{\boldsymbol{h}}^\star_i := \frac{1}{K}\sum_{j=1}^{K} \boldsymbol{h}^\star_{j,i} = \mathbf{0}, \quad \forall\, i \in [n],
\end{aligned} \tag{4}
$$

where either $b^\star = 0$ or $\lambda_{\boldsymbol{b}} = 0$, and the matrix $\boldsymbol{W}^{\star\top} \in \mathbb{R}^{d\times K}$ forms a K-Simplex ETF (defined in Definition C.1) up to some scaling, in the sense that the normalized matrix $\boldsymbol{M} := \frac{1}{w^\star}\boldsymbol{W}^{\star\top}$ satisfies

$$
\boldsymbol{M}^\top \boldsymbol{M} = \frac{K}{K-1}\left(\boldsymbol{I}_K - \frac{1}{K}\mathbf{1}_K\mathbf{1}_K^\top\right). \tag{5}
$$

At a high level, our proof (in Appendix D) finds lower bounds for the loss in (3) and studies the conditions for the lower bounds to be achieved, similar to [24, 26]. As can be seen in this result, any global solution of the loss function (3) exhibits $\mathcal{NC}$ in the sense that the variability of output features $\{\boldsymbol{h}^\star_{k,i}\}_{i=1}^n$ of each class k ($1 \leq k \leq K$) collapses to zero, and any pair of features $(\boldsymbol{h}^\star_{k_1,i}, \boldsymbol{h}^\star_{k_2,j})$ from different classes $k_1 \neq k_2$ are maximally separated. Similar results have been obtained in [24–26], which considered different problem formulations, as we have discussed in Section 2.1.

- **Relationship between Class Number K and Feature Dimension d.** The requirement that $d \geq K-1$ is necessary for Theorem 3.1 to hold, simply because K vectors in $\mathbb{R}^d$ cannot form a K-Simplex ETF if $K > d+1$. However, the relationship $d \geq K$ is often true in practice. In general, and in overparameterized models in particular, the feature dimension, d, is significantly larger than the number of classes, K. For example, the dimension of the features of a ResNet [18] is typically set to $d = 512$ for CIFAR10 [21], a dataset with $K = 10$ classes. This dimension grows to $d = 2048$ for ImageNet [22], a dataset with $K = 1000$ classes.
- **Interpretations on the Bias Term $b^\star$.** In contrast to previous works [24–26], we consider the bias term in the unconstrained feature model (3). Our result indicates that a collapsing phenomenon also exists in the bias term $\boldsymbol{b}^\star$, in the sense that all the elements of $\boldsymbol{b}^\star$ are identical. When the features $\boldsymbol{H}$ are completely unconstrained, our result implies that removing the bias term $\boldsymbol{b}$ has no influence on the performance of the classifier. However, it should be noted that the ReLU unit is often applied at the end of the penultimate layer, so that $\boldsymbol{H}$ should be constrained to be nonnegative, $\boldsymbol{H} \geq \mathbf{0}$. In such cases, $\overline{\boldsymbol{h}}^\star_i$ will no longer be zero, and neither will $\boldsymbol{b}^\star$. Here, the bias

term $\boldsymbol{b}^\star$ will compensate for the global mean of the features, so that the globally-centered features still form a Simplex ETF [1].[10]

3.1 Characterizations of the Benign Global Landscape for (3)

The global optimality condition in Theorem 3.1 does not necessarily mean that we can achieve these global solutions efficiently, as the problem is still nonconvex. We now investigate the global optimization landscape of (3) by characterizing all of its critical points. Our next result implies that the training loss is a strict saddle function, and every critical point is either a global minimizer or a strict saddle point that can be escaped using negative curvatures. As a consequence, this implies that the global solutions of the training problem in (3) can be efficiently found from random initializations.

Theorem 3.2 (No Spurious Local Minima and Strict Saddle Property) *Assume that the feature dimension is larger than the number of classes, $d > K$, and the number of training samples in each class is balanced $n = n_1 = \cdots = n_K$. Then the function $f(\boldsymbol{W}, \boldsymbol{H}, \boldsymbol{b})$ in (3) is a strict saddle function with no spurious local minimum, in the sense that*

- *Any local minimizer of (3) is a global minimizer of the form shown in Theorem 3.1.*
- *Any critical point $(\boldsymbol{W}, \boldsymbol{H}, \boldsymbol{b})$ of (3) that is not a local minimizer is a strict saddle with negative curvature, i.e. the Hessian $\nabla^2 f(\boldsymbol{W}, \boldsymbol{H}, \boldsymbol{b})$, at this critical point, is non-degenerate and has at least one negative eigenvalue, i.e. $\exists\, i:\ \lambda_i \left(\nabla^2 f(\boldsymbol{W}, \boldsymbol{H}, \boldsymbol{b})\right) < 0$.*

In a nutshell, our proof relies on connecting the original nonconvex optimization problem (3) to its corresponding low-rank convex counterpart, so that we can obtain the global optimality conditions for (3) based on the latter. With this, we can then characterize the properties of all critical points based on the optimality conditions. We defer all details of this proof to Appendix D.

Existing results [24–26] have *only* studied the global minimizers of the original problem, which has limited implication for optimization. In contrast, Theorem 3.2 characterizes the properties for *all* critical points of the function in (3). As a consequence of this result, many first-order and second-order optimization methods [69] optimizing $(\boldsymbol{W}, \boldsymbol{H}, \boldsymbol{b})$ are guaranteed to converge to a global solution of (3). In particular, the result in [49, 52] ensures that (stochastic) gradient descent with random initialization, the *de facto* optimization algorithm used in deep learning, almost surely escapes strict saddles and converges to a second-order critical point – which happens to be a global minimizer of form showed in Theorem 3.1 for our problem (3).

- **Constructing the Negative Curvature Direction for Strict Saddles.** One of the major difficulties in our proof is to construct the negative curvature direction for strict saddle points. Here, we exploit the fact that the feature dimension d is larger than the number of classes K, and construct the negative curvature direction within the null space of $\boldsymbol{W} \in \mathbb{R}^{K\times d}$. This is also the main reason for the requirement $d > K$ in Theorem 3.2, but we conjecture the results also hold for $d = K$ and could be proved with more sophisticated analysis, which is left as future work.
- **Relationship to Low-Rank Matrix Recovery.** As discussed in Appendix A, it has been recently shown that the strict saddle property holds for a wide range of nonconvex problems in machine learning [70–83], including low-rank matrix recovery [78, 80, 84–87]. As we know that $\|\boldsymbol{Z}\|_* = \min_{\boldsymbol{Z}=\boldsymbol{W}\boldsymbol{H}} \frac{1}{2}(\|\boldsymbol{W}\|_F^2 + \|\boldsymbol{H}\|_F^2)$ (see [32] for a proof), our formulation in (3) is closely related to low-rank matrix problems [78, 80, 84–87] with the Burer-Moneirto factorization approach [88], by viewing $\boldsymbol{W}$ and $\boldsymbol{H}$ as two factors of a matrix $\boldsymbol{Z} = \boldsymbol{W}\boldsymbol{H}$. The differences lie in the loss functions and statistical properties of the problem.[11] Thus, our result establishes a connection between the study of low-rank matrix factorization and neural networks under the unconstrained feature model.

[10] Suppose that an optimal solution to (3) is $(\boldsymbol{W}^\star, \boldsymbol{H}^\star, \boldsymbol{b}^\star)$, satisfying the conditions in Theorem 3.1. There exists a nonzero vector $\boldsymbol{\alpha} \in \mathbb{R}^d$ such that $\widetilde{\boldsymbol{H}}^\star = \boldsymbol{H}^\star + \boldsymbol{\alpha}\mathbf{1}^\top \geq 0$. Here, $\boldsymbol{\alpha}$ can be viewed as the global mean of $\widetilde{\boldsymbol{H}}^\star$ since $\boldsymbol{H}^\star$ has mean zero. Then, let $\widetilde{\boldsymbol{b}}^\star = -\boldsymbol{W}^\star\boldsymbol{\alpha}$, so that $\widetilde{\boldsymbol{W}}^\star\widetilde{\boldsymbol{H}}^\star + \widetilde{\boldsymbol{b}}^\star\mathbf{1}^\top = \boldsymbol{W}^\star\boldsymbol{H}^\star + (\boldsymbol{W}^\star\boldsymbol{\alpha} + \widetilde{\boldsymbol{b}}^\star)\mathbf{1}^\top = \boldsymbol{W}^\star\boldsymbol{H}^\star$. Therefore, we can see that $(\widetilde{\boldsymbol{W}}^\star, \widetilde{\boldsymbol{H}}^\star, \widetilde{\boldsymbol{b}}^\star)$ achieves the same cross-entropy loss as $(\boldsymbol{W}^\star, \boldsymbol{H}^\star, \boldsymbol{b}^\star)$.

[11] We consider the cross-entropy loss rather than the least-squares loss due to the differences in the task – we focus on classification instead of recovery problems. On the other hand, the results on low-rank matrix recovery are often based on certain statistical properties, such as the randomness in the measurements [84, 85], or restricted well-conditionedness property of the objective function [77, 87]. In contrast, these statistical properties do not exist in our problem, where the model and analysis are purely deterministic.

- **Comparison to Existing Landscape Analysis on Neural Network.** Section 1 provided a comprehensive discussion on the relationship between our result and previous works on landscape analysis for deep neural networks. Although the unconstrained feature model can be viewed as a two-layer linear network with input being the columns of an identity matrix, as preluded in Section 1, our result has much broader implications than the previous results [33,34,37,38,40,41,89]. First, our problem formulation (3) is closer to practical settings for classification tasks, which considers the widely adopted cross-entropy loss while including weight decay and a bias term, while most existing results [33,34,37,38,40,41,89] either do not incorporate any regularization and bias, or focus on the squared loss for the regression problem. More importantly, our result characterizes the precise form of the global solutions (i.e., $\mathcal{NC}$) for the last layer features and classifiers, and shows that they can be efficiently achieved. Moreover, convincing numerical results in [1] and the next section demonstrate that the global solutions do appear and can be achieved by practical networks on various standard image datasets. Our study of last-layer features could have profound implications for studying generalization and robustness of the deep networks.

4 Experiments

In this section, we run extensive experiments not only verifying our theoretical results on modern neural networks, but also demonstrating the potential practical benefits of understanding $\mathcal{NC}$. More specifically, while Theorem 3.2 holds true for the simplified unconstrained feature model, in Section 4.1 we run experiments on practical network architectures and show that our analysis of simplified models captures the gist of $\mathcal{NC}$. In particular, we demonstrate that this depends on the geometry of the problem rather than the algorithmic bias, by showing that different types of optimization algorithms *all* achieve $\mathcal{NC}$ during the terminal phase of training. In Section 4.2, we verify the validity of the simplification based on the unconstrained feature model. Moreover, the universality of $\mathcal{NC}$ implies that there is no need for training the last-layer classifiers since the weights can be simply fixed as a Simplex ETF throughout the training process. In Section 4.3, we demonstrate that such a strategy achieves essentially the same generalization performance as classical training algorithms, while improving on memory and computation. We begin by describing the basic experimental setup, including the network architectures, evaluation datasets, training procedures, and metrics for measuring $\mathcal{NC}$.

Setup of Network Architectures, Dataset, and Training. In Section 4.1 and Section 4.2, we train a ResNet18 architecture [18] on CIFAR10 [21] for image classification using the cross-entropy loss (2). Due to limited space, we present all the results on MNIST [90] in the Appendix. As is standard, images are normalized (channel-wise) by their mean and standard deviation. We include no data augmentation in this section, as our focus is to study the behavior associated with $\mathcal{NC}$ instead of obtaining state-of-the-art performance. We train the network for 200 epochs with three distinct optimizers: two first-order methods (SGD and Adam) and one second-order method (LBFGS [69]). In particular, we use SGD with momentum 0.9, Adam with $\beta_1 = 0.9, \beta_2 = 0.999$, and LBFGS with a memory size of 10. The initial learning rates for SGD and Adam are set to 0.05 and 0.001, respectively, and decreased by a factor of 10 for every 40 epochs. For LBFGS, we use an initial learning rate of 0.1 and employ a strong Wolfe line-search strategy for subsequent iterations. Except otherwise specified, the weight decay is set to 5×10^{-4} for all the experiments.

Metrics for Measuring $\mathcal{NC}$ During Network Training. We measure $\mathcal{NC}$ for the learned last-layer classifiers and features based on the properties presented in Section 1. Some of the metrics are similar to those presented in [1]. We first measure the within-class variability collapse by measuring the magnitude of the between-class covariance $\boldsymbol{\Sigma}_B \in \mathbb{R}^{d\times d}$ compared to the within-class covariance $\boldsymbol{\Sigma}_W \in \mathbb{R}^{d\times d}$ of the learned features via $\mathcal{NC}_1 := \frac{1}{K}\operatorname{trace}(\boldsymbol{\Sigma}_W \boldsymbol{\Sigma}_B^{\dagger})$, where $\boldsymbol{\Sigma}_B^{\dagger}$ denotes the pseudo inverse of $\boldsymbol{\Sigma}_B$. For the learned classifier $\boldsymbol{W} \in \mathbb{R}^{K\times d}$, we quantify its closeness to a Simplex ETF up to scaling by $\mathcal{NC}_2 := \left\| \frac{\boldsymbol{W}\boldsymbol{W}^\top}{\|\boldsymbol{W}\boldsymbol{W}^\top\|_F} - \frac{1}{\sqrt{K-1}}\left(\boldsymbol{I}_K - \frac{1}{K}\mathbf{1}_K\mathbf{1}_K^\top\right)\right\|_F$, where we rescale the ETF in (5) so that $\frac{1}{\sqrt{K-1}}(\boldsymbol{I}_K - \frac{1}{K}\mathbf{1}_K\mathbf{1}_K^\top)$ has unit energy (in Frobenius norm). It should be noted that our metric $\mathcal{NC}_2$ combines two metrics used in [1] to quantify to what extent the classifier approaches equiangularity and maximal-angle equiangularity. We then measure the duality between the classifiers $\boldsymbol{W}$ and the centered class-means $\overline{\boldsymbol{H}}$ by $\mathcal{NC}_3 := \left\| \frac{\boldsymbol{W}\overline{\boldsymbol{H}}}{\|\boldsymbol{W}\overline{\boldsymbol{H}}\|_F} - \frac{1}{\sqrt{K-1}}(\boldsymbol{I}_K - \frac{1}{K}\mathbf{1}_K\mathbf{1}_K^\top)\right\|_F$.

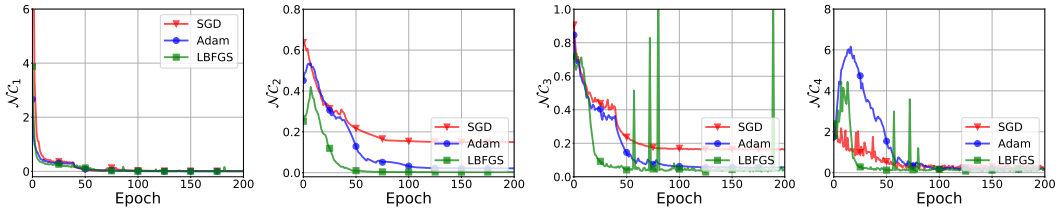

Figure 3: **Illustration of $\mathcal{NC}$ across different training algorithms** with ResNet18 on CIFAR10. From the left to the right, the plots show the four metrics, $\mathcal{NC}_1, \mathcal{NC}_2, \mathcal{NC}_3$, and $\mathcal{NC}_4$, respectively.

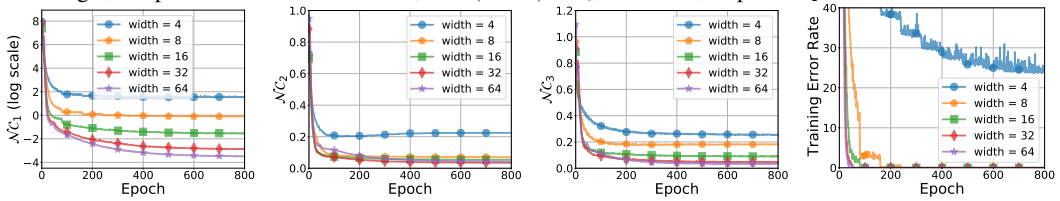

Figure 4: **Training results of ResNet18 with various feature width on CIFAR10 with completely random label.** From the left to the right: $\mathcal{NC}_1, \mathcal{NC}_2, \mathcal{NC}_3$, and the misclassification percentage of training samples.

In many cases, the global mean $\boldsymbol{h}_G$ of the features might not be zero,[12] and the bias term $\boldsymbol{b}$ would compensate for the global mean $\boldsymbol{h}_G$. Thus, we capture this collapsing phenomenon by measuring $\mathcal{NC}_4 := \|\boldsymbol{b} + \boldsymbol{W}\boldsymbol{h}_G\|_2$. The detailed descriptions of the four metrics are given in Appendix B.

4.1 The Prevalence of $\mathcal{NC}$ Across Different Optimization Algorithms

We show different types of training methods (e.g., SGD, Adam, and LBFGS) all achieve $\mathcal{NC}$ during the terminal phase of training. Figure 3 shows the evolution of the four metrics $\mathcal{NC}_1, \mathcal{NC}_2, \mathcal{NC}_3$, and $\mathcal{NC}_4$, for measuring $\mathcal{NC}$ as training progresses. We consistently observe that all four metrics collapse to zero, trained by different types of algorithms. This implies that $\mathcal{NC}$ occurs regardless of the choice of training methods. The last-layer features learned by the network are always maximally linearly separable, and correspondingly the last-layer classifier is a perfect linear classifier for the features. See Appendix for the testing performance of the networks learned by different algorithms.

4.2 The Validity of (3) Based on Unconstrained Feature Models for $\mathcal{NC}$

The premise of our global landscape analysis of (3) for studying $\mathcal{NC}$ in deep neural networks is based upon the unconstrained feature model introduced in Section 2.1, which simplifies the network by synthesizing the first $L-1$ layers as a universal approximator that generates a simple decision variable for each training sample. Here, we demonstrate through experiments that such a simplification is reasonable for overparameterized networks, in the sense that they are sufficient for characterizing $\mathcal{NC}$ in practical network training. In particular, we demonstrate that overparameterization is crucial for $\mathcal{NC}$ phenomenon during network training, while the input plays minimal influence. To that goal, we modify the training dataset CIFAR10 by replacing *all* the correct label for each training sample with a *random* counterpart.[13] We report the corresponding $\mathcal{NC}$ behaviors in Figure 4, which shows how training misclassification rate and $\mathcal{NC}$ evolve over epochs of training for networks with different widths[14]. As the network is sufficiently large, it has enough capacity to memorize the training data and achieves zero training error, which is consistent with the observations in [11]. Moreover, we find from Figure 4 that the training accuracy is highly correlated with $\mathcal{NC}$ in the sense that a larger network (i.e., larger width) tends to exhibit severe $\mathcal{NC}$ and achieves smaller training error. In other words, while the emerging consensus is that the network can interpolate any training data, our results show that such interpolation happens in a particular way – the features are maximally separated, followed by a max-margin linear classifier. In Appendix B, we also report experiments on weight decay imposed on the features $\boldsymbol{H}$, as in (3).

[12] For example, as discussed after Theorem 3.1 all the feature vectors in $\boldsymbol{H}$ would be nonnegative, because the nonnegative nonlinear operator ReLU has been applied at the end of the penultimate layer.

[13] We also conducted experiments on completely random dataset where each training image is generated with pixels uniformly from $[0, 1]$ and we observed similar results.

[14] Here, for ResNet18 we adopt the method in [15] to change its network width.

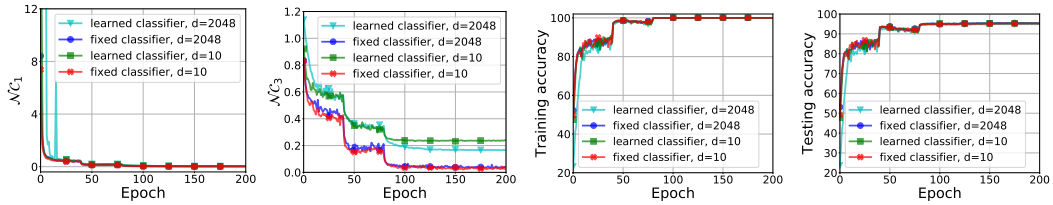

Figure 5: **Comparison of the performances of ResNet 50 with learned vs. fixed last-layer classifiers on CIFAR10.** From left to right): $\mathcal{NC}_1$, $\mathcal{NC}_3$, Training Accuracy, Testing Accuracy.

4.3 Insights from $\mathcal{NC}$ for Improving Network Designs

Finally, we conduct exploratory experiments to demonstrate the practical benefits of $\mathcal{NC}$ phenomenon. The universality of $\mathcal{NC}$ implies that the final classifier (i.e. the L-th layer) of a neural network always converges to a Simplex ETF, which is fully determined up to an arbitrary rotation and happens when $K \leq d$. Thus, based on these understandings, we show that we can substantially improve the computational cost by modifying the architecture without the sacrificing performance, by *(i)* fixing the last-layer classifier as a Simplex ETF[15], and *(ii)* reducing the feature dimension $d = K$. Here, to demonstrate our method can achieve state-of-the-art performance, we do include data augmentation in the training of our ResNet50 model [91] on CIFAR10, achieving around 95% test accuracy. See Appendix B for the results on MNIST and CIFAR10 with ResNet18.

Fixing the Last-layer Classifier as a Simplex ETF. Figure 5 presents a comparison of learned and fixed classifiers in terms of within-class variation collapse ($\mathcal{NC}_1$), self-duality ($\mathcal{NC}_3$), training accuracy, and test accuracy. These results imply that the fixed classifier exhibits the same within-class variation collapse for the features $\boldsymbol{H}$, and achieves the same classification accuracy as the *fully-trained* classifier. On the other hand, fixing the classifier can reduce the number of parameters and the computational complexity for training. The number of parameters in the classifier can be significant for tasks with a large number of classes and large feature dimensions. For example, for ImageNet, a dataset with $K = 1000$ classes, fixing the classifier can reduce 8.01%, 11.76%, and 52.56% of total learning parameters for ResNet50, DenseNet169 [19], and ShuffleNet [92], respectively. We note that our result also provides a theoretical justification for the work in [93] that fixes the classifier as orthonormal matrices. Indeed, these are close to simplex ETFs, particularly when the number of classes is large.

Feature Dimension Reduction for $\boldsymbol{H} \in \mathbb{R}^{d \times nK}$ by Choosing $d = K$.[16] In many classification problems, the practice of deep learning typically uses a feature dimension d that is much larger than the number of classes K. In contrast, $\mathcal{NC}$ implies that there is no need to choose a d that is much larger than the number of classes K. Reducing the dimension d can lead to substantial reductions in memory and computation cost. As shown in Figure 5, we also train all the weights of ResNet50 on CIFAR10 using SGD with $d = K$. The results demonstrate that $\mathcal{NC}$ persists even when we choose $d = K$, and the network achieves on-par performance with networks of large d, in terms of training and test accuracy. This implies that when the number of classes K is small, we can choose a small feature dimension $d = K$ (or $d \gtrsim K$) instead of using a large universal d to reduce the computation and memory costs for training. By setting $d = K$, this reduces the amount of parameters and hence the memory cost in ResNet18 and ResNet50 by 20.70% and 4.45% respectively.

5 Conclusion

In this work, we have provided an in-depth analysis to demystify the $\mathcal{NC}$ phenomenon, which appears during the terminal phase of training deep networks in classification problems. Based on the unconstrained feature model [24–26], we proved that Simplex ETFs are the only global minimizers of the cross-entropy training loss with weight decay and bias. Moreover, we showed that the loss function is a strict saddle function with respect to the last-layer features and classifiers, with no other spurious local minimizers. In contrast to existing landscape analyses for deep neural networks, which mostly focus on the optimization perspective, our simplified analysis not only characterizes

[15] Specifically, we set $\boldsymbol{W}^\top = \sqrt{\frac{K}{K-1}}\boldsymbol{P}\left(\boldsymbol{I}_K - \frac{1}{K}\mathbf{1}_K\mathbf{1}_K^\top\right)$ where $\boldsymbol{P} \in \mathbb{R}^{d \times K}$ contains the first K columns of a $d \times d$ identity matrix, which lifts a $K \times K$ ETF to $d \times K$ matrix. For simplicity, we also learn the bias term in the last layer, though our result indicates it can be set as $\boldsymbol{W}\overline{\boldsymbol{h}}$, where $\overline{\boldsymbol{h}}$ is the global mean of the features.

[16] Though Theorem 3.2 requires $d > K$, we conjecture it also holds for $d = K$ as discussed in Section 3.1.

the features that are learned in the last layer, but also explains why they can be efficiently optimized. This provides support for empirical observations in practical deep network architectures. Moreover, the study of last-layer features could have profound implications for optimization, generalization, and robustness of broad interests, which are the subjects of future work. It is also of interest to extend the current study to the case where $d < K$, which is the case in contrastive learning [94, 95] and many applications, such as recommendation systems [96] and document retrieval [97].

Acknowledgment

ZZ acknowledges support from NSF grant CCF 2008460. XL and QQ acknowledge support from NSF grant DMS 2009752. JS acknowledges support from NSF grant CCF 2007649. We would like to thank Qinqing Zheng (Facebook AI Research), Vardan Papyan (U. Toronto), and Felix Yu (Google Research) for timely pointing us to some important references and valuable feedback on the final draft. We thank Christina Baek (UC Berkeley) and Sam Buchanan (Columbia U.) for fruitful discussions during various stages of the work. We also thank Zhexin Wu (U. Michigan) for proofreading and pointing out several typos in the draft, and the four anonymous reviewers for their constructive comments.

References

[1] Vardan Papyan, XY Han, and David L Donoho. Prevalence of neural collapse during the terminal phase of deep learning training. *Proceedings of the National Academy of Sciences*, 117(40):24652–24663, 2020.

[2] Alex Krizhevsky, Ilya Sutskever, and Geoffrey E Hinton. Imagenet classification with deep convolutional neural networks. In *Advances in neural information processing systems*, pages 1097–1105, 2012.

[3] Yann LeCun, Yoshua Bengio, and Geoffrey Hinton. Deep learning. *nature*, 521(7553):436–444, 2015.

[4] Ian Goodfellow, Yoshua Bengio, Aaron Courville, and Yoshua Bengio. *Deep learning*, volume 1. MIT press Cambridge, 2016.

[5] Andrew W Senior, Richard Evans, John Jumper, James Kirkpatrick, Laurent Sifre, Tim Green, Chongli Qin, Augustin Žídek, Alexander WR Nelson, Alex Bridgland, et al. Improved protein structure prediction using potentials from deep learning. *Nature*, 577(7792):706–710, 2020.

[6] Behnam Neyshabur, Ryota Tomioka, and Nathan Srebro. In search of the real inductive bias: On the role of implicit regularization in deep learning. *arXiv preprint arXiv:1412.6614*, 2014.

[7] Daniel Soudry, Elad Hoffer, Mor Shpigel Nacson, Suriya Gunasekar, and Nathan Srebro. The implicit bias of gradient descent on separable data. *The Journal of Machine Learning Research*, 19(1):2822–2878, 2018.

[8] Sanjeev Arora, Nadav Cohen, Wei Hu, and Yuping Luo. Implicit regularization in deep matrix factorization. *Advances in Neural Information Processing Systems*, 32, 2019.

[9] Edward Moroshko, Blake E Woodworth, Suriya Gunasekar, Jason D Lee, Nati Srebro, and Daniel Soudry. Implicit bias in deep linear classification: Initialization scale vs training accuracy. *Advances in Neural Information Processing Systems*, 33, 2020.

[10] Noam Razin and Nadav Cohen. Implicit regularization in deep learning may not be explainable by norms. *Advances in Neural Information Processing Systems*, 33, 2020.

[11] Chiyuan Zhang, Samy Bengio, Moritz Hardt, Benjamin Recht, and Oriol Vinyals. Understanding deep learning requires rethinking generalization. *arXiv preprint arXiv:1611.03530*, 2016.

[12] Mikhail Belkin, Daniel Hsu, Siyuan Ma, and Soumik Mandal. Reconciling modern machine-learning practice and the classical bias–variance trade-off. *Proceedings of the National Academy of Sciences*, 116(32):15849–15854, 2019.

[13] Song Mei and Andrea Montanari. The generalization error of random features regression: Precise asymptotics and double descent curve. *arXiv preprint arXiv:1908.05355*, 2019.

[14] Preetum Nakkiran, Gal Kaplun, Yamini Bansal, Tristan Yang, Boaz Barak, and Ilya Sutskever. Deep double descent: Where bigger models and more data hurt. *arXiv preprint arXiv:1912.02292*, 2019.

[15] Zitong Yang, Yaodong Yu, Chong You, Jacob Steinhardt, and Yi Ma. Rethinking bias-variance trade-off for generalization of neural networks. In *International Conference on Machine Learning*, pages 10767–10777. PMLR, 2020.

[16] Vardan Papyan. Traces of class/cross-class structure pervade deep learning spectra. *Journal of Machine Learning Research*, 21(252):1–64, 2020.

[17] Karen Simonyan and Andrew Zisserman. Very deep convolutional networks for large-scale image recognition. *arXiv preprint arXiv:1409.1556*, 2014.

[18] Kaiming He, Xiangyu Zhang, Shaoqing Ren, and Jian Sun. Deep residual learning for image recognition. In *Proceedings of the IEEE conference on computer vision and pattern recognition*, pages 770–778, 2016.

[19] Gao Huang, Zhuang Liu, Laurens Van Der Maaten, and Kilian Q Weinberger. Densely connected convolutional networks. In *Proceedings of the IEEE conference on computer vision and pattern recognition*, pages 4700–4708, 2017.

[20] Yann LeCun, Corinna Cortes, and CJ Burges. Mnist handwritten digit database. at&t labs, 2010.

[21] Alex Krizhevsky, Geoffrey Hinton, et al. Learning multiple layers of features from tiny images. 2009.

[22] Jia Deng, Wei Dong, Richard Socher, Li-Jia Li, Kai Li, and Li Fei-Fei. Imagenet: A large-scale hierarchical image database. In *2009 IEEE conference on computer vision and pattern recognition*, pages 248–255. Ieee, 2009.

[23] Dustin G Mixon, Hans Parshall, and Jianzong Pi. Neural collapse with unconstrained features. *arXiv preprint arXiv:2011.11619*, 2020.

[24] Jianfeng Lu and Stefan Steinerberger. Neural collapse with cross-entropy loss. *arXiv preprint arXiv:2012.08465*, 2020.

[25] E Weinan and Stephan Wojtowytsch. On the emergence of tetrahedral symmetry in the final and penultimate layers of neural network classifiers. *arXiv preprint arXiv:2012.05420*, 2020.

[26] Cong Fang, Hangfeng He, Qi Long, and Weijie J Su. Layer-peeled model: Toward understanding well-trained deep neural networks. *arXiv preprint arXiv:2101.12699*, 2021.

[27] Florian Graf, Christoph Hofer, Marc Niethammer, and Roland Kwitt. Dissecting supervised constrastive learning. In *International Conference on Machine Learning*, pages 3821–3830. PMLR, 2021.

[28] Tolga Ergen and Mert Pilanci. Revealing the structure of deep neural networks via convex duality. In *International Conference on Machine Learning*, pages 3004–3014. PMLR, 2021.

[29] John Zarka, Florentin Guth, and Stéphane Mallat. Separation and concentration in deep networks. *arXiv preprint arXiv:2012.10424*, 2020.

[30] Yaodong Yu, Kwan Ho Ryan Chan, Chong You, Chaobing Song, and Yi Ma. Learning diverse and discriminative representations via the principle of maximal coding rate reduction. *arXiv preprint arXiv:2006.08558*, 2020.

[31] Kwan Ho Ryan Chan, Yaodong Yu, Chong You, Haozhi Qi, John Wright, and Yi Ma. Deep networks from the principle of rate reduction. *arXiv preprint arXiv:2010.14765*, 2020.

[32] Benjamin D Haeffele and René Vidal. Global optimality in tensor factorization, deep learning, and beyond. *arXiv preprint arXiv:1506.07540*, 2015.

[33] Pierre Baldi and Kurt Hornik. Neural networks and principal component analysis: Learning from examples without local minima. *Neural networks*, 2(1):53–58, 1989.

[34] Kenji Kawaguchi. Deep learning without poor local minima. *Advances in neural information processing systems*, 29:586–594, 2016.

[35] Itay Safran and Ohad Shamir. Spurious local minima are common in two-layer relu neural networks. In *International Conference on Machine Learning*, pages 4433–4441. PMLR, 2018.

[36] Chulhee Yun, Suvrit Sra, and Ali Jadbabaie. Small nonlinearities in activation functions create bad local minima in neural networks. In *International Conference on Learning Representations*, 2018.

[37] Thomas Laurent and James Brecht. Deep linear networks with arbitrary loss: All local minima are global. In *International conference on machine learning*, pages 2902–2907. PMLR, 2018.

[38] Maher Nouiehed and Meisam Razaviyayn. Learning deep models: Critical points and local openness. *arXiv preprint arXiv:1803.02968*, 2018.

[39] Shiyu Liang, Ruoyu Sun, Jason D Lee, and R Srikant. Adding one neuron can eliminate all bad local minima. *Advances in Neural Information Processing Systems*, 2018:4350–4360, 2018.

[40] Zhihui Zhu, Daniel Soudry, Yonina C Eldar, and Michael B Wakin. The global optimization geometry of shallow linear neural networks. *Journal of Mathematical Imaging and Vision*, pages 1–14, 2019.

[41] Chulhee Yun, Suvrit Sra, and Ali Jadbabaie. Global optimality conditions for deep neural networks. In *International Conference on Learning Representations*, 2018.

[42] Mo Zhou, Rong Ge, and Chi Jin. A local convergence theory for mildly over-parameterized two-layer neural network. *arXiv preprint arXiv:2102.02410*, 2021.

[43] G Cybenko. Approximation by superposition of sigmoidal functions. *Mathematics of Control, Signals and Systems*, 2(4):303–314, 1989.

[44] Kurt Hornik. Approximation capabilities of multilayer feedforward networks. *Neural networks*, 4(2):251–257, 1991.

[45] Zhou Lu, Hongming Pu, Feicheng Wang, Zhiqiang Hu, and Liwei Wang. The expressive power of neural networks: a view from the width. In *Proceedings of the 31st International Conference on Neural Information Processing Systems*, pages 6232–6240, 2017.

[46] Uri Shaham, Alexander Cloninger, and Ronald R Coifman. Provable approximation properties for deep neural networks. *Applied and Computational Harmonic Analysis*, 44(3):537–557, 2018.

[47] XY Han, Vardan Papyan, and David L Donoho. Neural collapse under mse loss: Proximity to and dynamics on the central path. *arXiv preprint arXiv:2106.02073*, 2021.

[48] Wenlong Ji, Yiping Lu, Yiliang Zhang, Zhun Deng, and Weijie J Su. An unconstrained layer-peeled perspective on neural collapse. *arXiv preprint arXiv:2110.02796*, 2021.

[49] Rong Ge, Furong Huang, Chi Jin, and Yang Yuan. Escaping from saddle points—online stochastic gradient for tensor decomposition. In *Proceedings of The 28th Conference on Learning Theory*, pages 797–842, 2015.

[50] Ju Sun, Qing Qu, and John Wright. When are nonconvex problems not scary? *arXiv preprint arXiv:1510.06096*, 2015.

[51] Yuqian Zhang, Qing Qu, and John Wright. From symmetry to geometry: Tractable nonconvex problems. *arXiv preprint arXiv:2007.06753*, 2020.

[52] Jason D Lee, Max Simchowitz, Michael I Jordan, and Benjamin Recht. Gradient descent only converges to minimizers. In *Conference on learning theory*, pages 1246–1257. PMLR, 2016.

[53] Michael Elad, Dror Simon, and Aviad Aberdam. Another step toward demystifying deep neural networks. *Proceedings of the National Academy of Sciences*, 117(44):27070–27072, 2020.

[54] Suriya Gunasekar, Jason Lee, Daniel Soudry, and Nathan Srebro. Implicit bias of gradient descent on linear convolutional networks. *In Advances in Neural Information Processing Systems*, 2018.

[55] Gauthier Gidel, Francis Bach, and Simon Lacoste-Julien. Implicit regularization of discrete gradient dynamics in linear neural networks. In H. Wallach, H. Larochelle, A. Beygelzimer, F. d'Alché-Buc, E. Fox, and R. Garnett, editors, *Advances in Neural Information Processing Systems*, volume 32, 2019.

[56] Mor Shpigel Nacson, Jason Lee, Suriya Gunasekar, Pedro Henrique Pamplona Savarese, Nathan Srebro, and Daniel Soudry. Convergence of gradient descent on separable data. In *The 22nd International Conference on Artificial Intelligence and Statistics*, pages 3420–3428. PMLR, 2019.

[57] Ziwei Ji, Miroslav Dudík, Robert E Schapire, and Matus Telgarsky. Gradient descent follows the regularization path for general losses. In *Conference on Learning Theory*, pages 2109–2136. PMLR, 2020.

[58] Kaifeng Lyu and Jian Li. Gradient descent maximizes the margin of homogeneous neural networks. In *International Conference on Learning Representations*, 2019.

[59] Ohad Shamir. Gradient methods never overfit on separable data. *Journal of Machine Learning Research*, 22(85):1–20, 2021.

[60] Meena Jagadeesan, Ilya Razenshteyn, and Suriya Gunasekar. Inductive bias of multi-channel linear convolutional networks with bounded weight norm. *arXiv preprint arXiv:2102.12238*, 2021.

[61] Chong You, Zhihui Zhu, Qing Qu, and Yi Ma. Robust recovery via implicit bias of discrepant learning rates for double over-parameterization. In H. Larochelle, M. Ranzato, R. Hadsell, M. F. Balcan, and H. Lin, editors, *Advances in Neural Information Processing Systems*, volume 33, pages 17733–17744. Curran Associates, Inc., 2020.

[62] John Duchi, Elad Hazan, and Yoram Singer. Adaptive subgradient methods for online learning and stochastic optimization. *Journal of machine learning research*, 12(7), 2011.

[63] Diederik P Kingma and Jimmy Ba. Adam: A method for stochastic optimization. *arXiv preprint arXiv:1412.6980*, 2014.

[64] Mor Shpigel Nacson, Nathan Srebro, and Daniel Soudry. Stochastic gradient descent on separable data: Exact convergence with a fixed learning rate. In *The 22nd International Conference on Artificial Intelligence and Statistics*, pages 3051–3059. PMLR, 2019.

[65] Qian Qian and Xiaoyuan Qian. The implicit bias of adagrad on separable data. *arXiv preprint arXiv:1906.03559*, 2019.

[66] Suriya Gunasekar, Jason Lee, Daniel Soudry, and Nathan Srebro. Characterizing implicit bias in terms of optimization geometry. In *International Conference on Machine Learning*, pages 1832–1841. PMLR, 2018.

[67] Vinod Nair and Geoffrey Hinton. Rectified linear units improve restricted boltzmann machines. volume 27, pages 807–814, 2010.

[68] Sergey Ioffe and Christian Szegedy. Batch normalization: Accelerating deep network training by reducing internal covariate shift. In *ICML*, pages 448–456, 2015.

[69] Léon Bottou, Frank E Curtis, and Jorge Nocedal. Optimization methods for large-scale machine learning. *Siam Review*, 60(2):223–311, 2018.

[70] Qing Qu, Ju Sun, and John Wright. Finding a sparse vector in a subspace: Linear sparsity using alternating directions. In *Advances in Neural Information Processing Systems*, pages 3401–3409, 2014.

[71] Tuo Zhao, Zhaoran Wang, and Han Liu. A nonconvex optimization framework for low rank matrix estimation. In *Advances in Neural Information Processing Systems*, pages 559–567, 2015.

[72] Ju Sun, Qing Qu, and John Wright. Complete dictionary recovery over the sphere I: Overview and the geometric picture. *IEEE Transactions on Information Theory*, 63(2):853–884, 2016.

[73] Ju Sun, Qing Qu, and John Wright. Complete dictionary recovery over the sphere II: Recovery by Riemannian trust−region method. *IEEE Transactions on Information Theory*, 63(2):853–884, 2017.

[74] Qiuwei Li, Zhihui Zhu, and Gongguo Tang. The non-convex geometry of low-rank matrix optimization. *Information and Inference: A Journal of the IMA*, 8(1):51–96, 2018.

[75] Qing Qu, Yuqian Zhang, Yonina Eldar, and John Wright. Convolutional phase retrieval. In *Advances in Neural Information Processing Systems*, pages 6086–6096, 2017.

[76] Ju Sun, Qing Qu, and John Wright. A geometric analysis of phase retrieval. *Foundations of Computational Mathematics*, 18(5):1131–1198, 2018.

[77] Zhihui Zhu, Qiuwei Li, Gongguo Tang, and Michael B Wakin. Global optimality in low-rank matrix optimization. *IEEE Transactions on Signal Processing*, 66(13):3614–3628, 2018.

[78] Xingguo Li, Junwei Lu, Raman Arora, Jarvis Haupt, Han Liu, Zhaoran Wang, and Tuo Zhao. Symmetry, saddle points, and global optimization landscape of nonconvex matrix factorization. *IEEE Transactions on Information Theory*, 65(6):3489–3514, 2019.

[79] Zhihui Zhu, Qiuwei Li, Xinshuo Yang, Gongguo Tang, and Michael B Wakin. Distributed low-rank matrix factorization with exact consensus. In *Advances in Neural Information Processing Systems*, pages 8422–8432, 2019.

[80] Yuejie Chi, Yue M Lu, and Yuxin Chen. Nonconvex optimization meets low-rank matrix factorization: An overview. *IEEE Transactions on Signal Processing*, 67(20):5239–5269, 2019.

[81] Qing Qu, Yuexiang Zhai, Xiao Li, Yuqian Zhang, and Zhihui Zhu. Geometric analysis of nonconvex optimization landscapes for overcomplete learning. In *International Conference on Learning Representations*, 2020.

[82] Qing Qu, Zhihui Zhu, Xiao Li, Manolis C. Tsakiris, John Wright, and René Vidal. Finding the sparsest vectors in a subspace: Theory, algorithms, and applications. *arXiv preprint arXiv:2001.06970*, 2020.

[83] Qing Qu, Xiao Li, and Zhihui Zhu. Exact recovery of multichannel sparse blind deconvolution via gradient descent. *SIAM Journal on Imaging Sciences*, 13(3):1630–1652, 2020.

[84] Rong Ge, Jason D Lee, and Tengyu Ma. Matrix completion has no spurious local minimum. *arXiv preprint arXiv:1605.07272*, 2016.

[85] Srinadh Bhojanapalli, Behnam Neyshabur, and Nathan Srebro. Global optimality of local search for low rank matrix recovery. In *Proceedings of the 30th International Conference on Neural Information Processing Systems*, pages 3880–3888, 2016.

[86] Rong Ge, Chi Jin, and Yi Zheng. No spurious local minima in nonconvex low rank problems: A unified geometric analysis. In *International Conference on Machine Learning*, pages 1233–1242. PMLR, 2017.

[87] Qiuwei Li, Zhihui Zhu, and Gongguo Tang. The non-convex geometry of low-rank matrix optimization. *Information and Inference: A Journal of the IMA*, 8(1):51–96, 2019.

[88] Samuel Burer and Renato DC Monteiro. A nonlinear programming algorithm for solving semidefinite programs via low-rank factorization. *Mathematical Programming*, 95(2):329–357, 2003.

[89] Daniel Kunin, Jonathan Bloom, Aleksandrina Goeva, and Cotton Seed. Loss landscapes of regularized linear autoencoders. In *International Conference on Machine Learning*, pages 3560–3569. PMLR, 2019.

[90] Yann LeCun. The mnist database of handwritten digits. *http://yann. lecun. com/exdb/mnist/*, 1998.

[91] kuang Liu, Wei Yang, Yang Peiwen, and Felipe Ducau. Train cifar10 with pytorch. https://github.com/kuangliu/pytorch-cifar/blob/master/models/resnet.py.

[92] Xiangyu Zhang, Xinyu Zhou, Mengxiao Lin, and Jian Sun. Shufflenet: An extremely efficient convolutional neural network for mobile devices. In *Proceedings of the IEEE conference on computer vision and pattern recognition*, pages 6848–6856, 2018.

[93] Elad Hoffer, Itay Hubara, and Daniel Soudry. Fix your classifier: the marginal value of training the last weight layer. In *International Conference on Learning Representations*, 2018.

[94] Ting Chen, Simon Kornblith, Mohammad Norouzi, and Geoffrey Hinton. A simple framework for contrastive learning of visual representations. *arXiv preprint arXiv:2002.05709*, 2020.

[95] Kaiming He, Haoqi Fan, Yuxin Wu, Saining Xie, and Ross Girshick. Momentum contrast for unsupervised visual representation learning. In *Proceedings of the IEEE/CVF Conference on Computer Vision and Pattern Recognition*, pages 9729–9738, 2020.

[96] Paul Covington, Jay Adams, and Emre Sargin. Deep neural networks for youtube recommendations. In *Proceedings of the 10th ACM conference on recommender systems*, pages 191–198, 2016.

[97] Wei-Cheng Chang, X Yu Felix, Yin-Wen Chang, Yiming Yang, and Sanjiv Kumar. Pre-training tasks for embedding-based large-scale retrieval. In *International Conference on Learning Representations*, 2019.

[98] Ruo-Yu Sun. Optimization for deep learning: An overview. *Journal of the Operations Research Society of China*, 8(2):249–294, 2020.

[99] Ruoyu Sun, Dawei Li, Shiyu Liang, Tian Ding, and Rayadurgam Srikant. The global landscape of neural networks: An overview. *IEEE Signal Processing Magazine*, 37(5):95–108, 2020.

[100] Zeyuan Allen-Zhu, Yuanzhi Li, and Zhao Song. A convergence theory for deep learning via over-parameterization. In *International Conference on Machine Learning*, pages 242–252, 2019.

[101] Simon Du, Jason Lee, Haochuan Li, Liwei Wang, and Xiyu Zhai. Gradient descent finds global minima of deep neural networks. In *International Conference on Machine Learning*, pages 1675–1685, 2019.

[102] Arthur Jacot, Clément Hongler, and Franck Gabriel. Neural tangent kernel: Convergence and generalization in neural networks. In *NeurIPS*, 2018.

[103] Difan Zou, Yuan Cao, Dongruo Zhou, and Quanquan Gu. Gradient descent optimizes over-parameterized deep relu networks. *Machine Learning*, 109(3):467–492, 2020.

[104] Andrea Montanari and Yiqiao Zhong. The interpolation phase transition in neural networks: Memorization and generalization under lazy training. *arXiv preprint arXiv:2007.12826*, 2020.

[105] Sam Buchanan, Dar Gilboa, and John Wright. Deep networks and the multiple manifold problem. *arXiv preprint arXiv:2008.11245*, 2020.

[106] Lénaïc Chizat, Edouard Oyallon, and Francis Bach. On lazy training in differentiable programming. *Advances in Neural Information Processing Systems*, 32:2937–2947, 2019.

[107] Marina Danilova, Pavel Dvurechensky, Alexander Gasnikov, Eduard Gorbunov, Sergey Guminov, Dmitry Kamzolov, and Innokentiy Shibaev. Recent theoretical advances in non-convex optimization. *arXiv preprint arXiv:2012.06188*, 2020.

[108] Chi Jin, Praneeth Netrapalli, Rong Ge, Sham M. Kakade, and Michael I. Jordan. On nonconvex optimization for machine learning: Gradients, stochasticity, and saddle points. *J. ACM*, 68(2), February 2021.

[109] Yenson Lau, Qing Qu, Han-Wen Kuo, Pengcheng Zhou, Yuqian Zhang, and John Wright. Short and sparse deconvolution — a geometric approach. In *International Conference on Learning Representations*, 2020.

[110] Han-Wen Kuo, Yenson Lau, Yuqian Zhang, and John Wright. Geometry and symmetry in short-and-sparse deconvolution. In *International Conference on Machine Learning*, pages 3570–3580. PMLR, 2019.

[111] Yuqian Zhang, Han-Wen Kuo, and John Wright. Structured local optima in sparse blind deconvolution. *IEEE Transactions on Information Theory*, 66(1):419–452, 2019.

[112] Raghu Bollapragada, Jorge Nocedal, Dheevatsa Mudigere, Hao-Jun Shi, and Ping Tak Peter Tang. A progressive batching l-bfgs method for machine learning. In *International Conference on Machine Learning*, pages 620–629. PMLR, 2018.

[113] Yi Ren and Donald Goldfarb. Kronecker-factored quasi-newton methods for convolutional neural networks. *arXiv preprint arXiv:2102.06737*, 2021.

[114] Roger A Horn and Charles R Johnson. *Matrix analysis*. Cambridge University Press, 2012.

[115] Carlo Ciliberto, Dimitris Stamos, and Massimiliano Pontil. Reexamining low rank matrix factorization for trace norm regularization. *arXiv preprint arXiv:1706.08934*, 2017.

[116] G Alistair Watson. Characterization of the subdifferential of some matrix norms. *Linear algebra and its applications*, 170:33–45, 1992.

[117] Benjamin Recht, Maryam Fazel, and Pablo A Parrilo. Guaranteed minimum-rank solutions of linear matrix equations via nuclear norm minimization. *SIAM Review*, 52(3):471–501, 2010.

Checklist

1. For all authors...
   (a) Do the main claims made in the abstract and introduction accurately reflect the paper's contributions and scope? [Yes]
   (b) Did you describe the limitations of your work? [Yes] In the abstract, introduction, main results, and conclusion, we explicitly stat that our results are about unconstrained feature model.
   (c) Did you discuss any potential negative societal impacts of your work? [N/A] This paper mainly focuses on understanding the neural collapse phenomena observed in practical neural networks. Based on this understanding, we propose to fix the last layer classifier as a Simplex ETF. So no potential negative societal impact is expected of this work.
   (d) Have you read the ethics review guidelines and ensured that your paper conforms to them? [Yes]
2. If you are including theoretical results...
   (a) Did you state the full set of assumptions of all theoretical results? [Yes] We explicitly mention the assumptions in Theorem 3.1 and Theorem 3.2.
   (b) Did you include complete proofs of all theoretical results? [Yes] We include all the proofs in the Appendix.
3. If you ran experiments...
   (a) Did you include the code, data, and instructions needed to reproduce the main experimental results (either in the supplemental material or as a URL)? [Yes] See Section 4 and Appendix.
   (b) Did you specify all the training details (e.g., data splits, hyperparameters, how they were chosen)? [Yes] See Section 4 and Appendix.
   (c) Did you report error bars (e.g., with respect to the random seed after running experiments multiple times)? [No] All the results are reported in terms of learning curves and each figure includes many plots, so error bars are not reported. Bud we do run the experiments multiple times, and observe very similar performance in terms of $\mathcal{NC}$, testing accuracy, etc.
   (d) Did you include the total amount of compute and the type of resources used (e.g., type of GPUs, internal cluster, or cloud provider)? [Yes] See Appendix B.
4. If you are using existing assets (e.g., code, data, models) or curating/releasing new assets...
   (a) If your work uses existing assets, did you cite the creators? [Yes] We cite them in Section 4.
   (b) Did you mention the license of the assets? [Yes] This is mentioned in Appendix B.
   (c) Did you include any new assets either in the supplemental material or as a URL? [N/A]
   (d) Did you discuss whether and how consent was obtained from people whose data you're using/curating? [Yes] This is discussed in Appendix B.
   (e) Did you discuss whether the data you are using/curating contains personally identifiable information or offensive content? [N/A]
5. If you used crowdsourcing or conducted research with human subjects...
   (a) Did you include the full text of instructions given to participants and screenshots, if applicable? [N/A]
   (b) Did you describe any potential participant risks, with links to Institutional Review Board (IRB) approvals, if applicable? [N/A]
   (c) Did you include the estimated hourly wage paid to participants and the total amount spent on participant compensation? [N/A]